Journal of Chemical Health Risks

www.jchr.org

ORIGINAL ARTICLE

Effects of Process Parameter on Crude Oil Biodegradation of Palm Oil Mill Effluent using Response Surface Optimization

Ani Kingsley Amechi[*1], Ezeugwu Felix [2]

[1] *Department of Chemical Engineering, Faculty of Engineering, Nnamdi Azikiwe University, P.M.B 5025, Awka, Anambra State, Nigeria*

[2] *Department of Science Laboratory Technology, Institute of Management and Technology Enugu P.M.B 1079, Enugu Nigeria*

(Received: 5 January 2019 Accepted: 19 April 2019)

KEYWORDS

Crude oil;
Contaminated soil;
Palm oil mill effluent;
First order kinetics;
second order kinetics;
Error analysis;
RSM

ABSTRACT: The aim of this study was to investigate the effects of process parameter on crude oil (CO) biodegradation of palm oil mill effluent (POME) by using response surface optimization. Physiochemical characterization of the uncontaminated soil (UCS), crude oil contaminated soils (COCS), and POME were investigated. Further characterization on the POME was done employing the scanning electron microscope (SEM) and Fourier transform infrared (FT-IR). First and second order kinetics models were used to estimate the kinetic parameters. Results obtained indicated that POME contained valuable soil nutrient as it showed a stimulatory effect on the physiochemical properties of the COCS. However, POME was able to degrade 51% of CO with an initial CO concentration of 130 g/L. The first order kinetics proved a better model with a high rate constant, lower biological half-life and R^2 greater than 0.96. From the optimization process, the quadratic model with 78.8% contribution and R^2 of 0.993 satisfactorily explained the interactions between the independent variable and the response. The FT-IR spectrum revealed the presence of nitrogen and phosphorous on the surface of POME, while SEM indicated a smooth surface of POME.

INTRODUCTION

The utilization of palm oil in various domestic and industrial processes to produce a number of products has contributed immensely to the global economy. Therefore, the need for the constant supply of palm oil in order to meet domestic and industrial needs cannot be overemphasized. However, one of the pressing challenges facing global palm oil production industries is on how to manage the huge wastes generated from palm oil extraction from fresh palm fruit bunches [1].

Nigeria alongside Indonesia, Malaysia, and Thailand produce palm oil for economic growth in large quantities. However, these countries are faced with the challenges of managing the numerous wastes generated from palm oil extraction such as the palm oil mill effluent (POME) [1]. Environmental issues as a result of POME discharge are increasingly becoming a source of concern in Nigeria. Due to the huge amount of water required for palm oil extraction, POME in most cases is discharged in nearby soil and/or water without treatment [2].

The indiscriminate discharge of POME from palm oil mill factories could contaminate underground water resources and destroy aquatic animals etc. However, existing researches are focused on the physicochemical treatments of POME like sedimentation by coagulation and flocculation [3] adsorption and membrane filtration

*Corresponding author: anikingsley16@yahoo.com (A. Kingsley Amechi)

[4]. There are growing interests in the utilization of POME for agricultural composting processes since POME are biological in nature and degradable [5].

Results from previous studies showed that POME contains a high concentration of organic matter [1]. Also, the application of POME to soil enriched the soil with Phosphorous, Nitrogen, Calcium and Magnesium which will lead to an improved soil fertility and sustainable environment [6]. However, the application of biologically treated POME for irrigation purposes and liquid fertilizer has been reported [7]. In a study carried out [8] to study the co-composting of POME with empty fruit bunch (EFB) on a pilot scale, authors reported that the pilot scale co-composting of POME with EFB gave acceptable quality of compost with considerably high amount of calcium, Nitrogen, Phosphorous, and Magnesium [8].

However, little or no information exists on the utilization of POME as an organic nutrient in crude oil contaminated soil (COCS), which was the focus of this study. Hence, the objectives of this study were to characterize the uncontaminated soil (UCS), COCS, and POME. Investigations were also carried out on the effects of POME on the COCS properties. Response surface optimization process was also employed to estimate the optimum conditions of the process variables in the COCS treated with POME (COCS-POME). Finally, the SEM and FT-IR were used to characterize POME.

MATERIALS AND METHODS

Samples Collection

The UCS used in this study was collected from the botanical garden of Nnamdi Azikiwe University Awka Anambra State Nigeria. The POME used in this study was collected from a palm oil mill factory located in Ogwofia-Ozom Mgbagbu Owa in Ezeagu Local Government Area of Enugu State Nigeria. The crude oil (CO) chosen as a choice contaminant to be monitored during the process was collected from Eleme Petrochemical refinery Port Harcourt Rivers State Nigeria. The samples were transported to the Soil Science Laboratory of the University of Nigeria Nsukka, Enugu State Nigeria for further analysis.

Samples Preparation

Stock solutions of the raw CO sample were prepared by weighing out (PCE analytical weighing balance PCE-6000) 50, 70, 90, 110 and 130 g of CO. Each of the mass of CO weighed out was diluted with 1.0 L of distilled water to give the desired CO concentrations (50, 70, 90, 110 and 130 g/L) range. The CO concentrations used were relatively low, due to the dilution process. The UCS and POME used in this study were air dried for 30 days to remove the inherent moisture. After drying, the samples were crushed and sieved using 2 mm particle size sieve, in order to obtain a homogenous sample and remove unwanted particles.

CO degradation procedure

The experimental procedure described in this section was carried out to study the effect of POME on the degradation of CO concentrations. 200 g of the UCS was placed in five plastic containers with dimensions of 60 x 40 cm. The prepared CO stock solutions in section 2.2 were used in contaminating the soil thereby creating an artificial COCS. The contaminated soil was thoroughly mixed with 100 g of POME at a constant ratio of 2:1 w/w, ensuring the homogeneity of the COCS and POME.

The containers were covered with a black polyethylene bag, in order to prevent the volatilization and photo-oxidation of the CO fractions [9]. Experimental control samples were used for comparative purposes. Distil water was used to adjust the water content of the treatment containers when necessary [10]. All experiments were carried out in duplicates and the statistical mean of the results obtained were recorded. The effectiveness of the CO degradation process was monitored by estimating CO degradation on a weekly basis during a 56 days remediation exercise using the expression in Eq. (1).

CO Analysis

In order to determine CO concentration in the treatment mixtures, solvent extraction method according to [10] was used. 10 g sub-samples were dried in an oven. The sub-samples were extracted using Soxhlet extraction process for three hours using acetone/dichloromethane

(1:1 v/v) as solvent. After the extraction process, the solvent was left evaporate. The remaining residue (extract) was dissolved in 5ml dichloromethane. The CO concentration was quantified using gas chromatography. The Gas chromatography was equipped with split less injector and flame ionization detector (FID). The initial temperature was maintained at 40°C for 2min before increasing it to 320°C at a rate of 7°C/min. The rate was increased to 20°C/min until the temperature reached 400°C and was kept constant for 10min. The recovery of CO using this method was higher than 65%. The CO concentrations were determined after calibration of the method with standard CO samples at different concentrations. The percentage of CO degraded was calculated using the expression in Eq. (1):

$$\%\text{CO degradation} = \frac{\text{initial COC} - \text{final COC}}{\text{initial COC}}\ x\ 100 \quad (1)$$

Where:

Initial COC is the Initial crude oil concentration

Final COC is the final crude oil concentration

Experimental design procedure

The central composite design (CCD) of response surface methodology (RSM) was employed to investigate the interaction and effect of the independent variables on CO degradation. These independent variables were pH (2 –10), Temperature (10 – 50°C) and CO concentration (50 – 130 g/L). The variables levels used in the statistical analysis of data were coded with the symbols −1, 0, and, 1 as shown in Table 1. MINITAB 17.0, which was the statistical software used in this study estimated the axial level (α) to be ±1.633 according to the number of experimental runs displayed.

Table 1. Levels of experimental variables

Variables	Symbol	Levels		
		minimum (-1)	medium (0)	maximum (1)
pH	A	2	6	10
Temperature (°C)	B	10	30	50
CO concentration (gL^{-1})	C	50	90	130

Table 2 presents the experimental design matrix which includes the variables combinations, responses, first and second order predicted responses. CCD was used to generate 20 experimental runs, which were carried out in a randomized order. A second-order quadratic model of (Eq. 2), which corresponds to the CCD of crude oil contaminated soil treated with POME (COCS-POME), was fitted to the CO degradation data using multiple regression method. This was in order to correlate the mathematical relationship between the independent variables and the response as presented in Eq. (2):

$$Y = \beta o + \sum_{i=1}^{n} \beta_j X_j + \sum_{i=1}^{n} \beta_{jj} X_j^{\,2} + \sum_{i=1}^{n-1} \sum_{j=2}^{n} \beta_{ij} X_i X_j \quad (2)$$

From Eq. (2), Y is the dependent variable (response), βo is the constant term, β_j, β_{jj}, and β_{ij} are the linear, quadratic and interaction coefficients, respectively. X_j, $X_j^{\,2}$ and X_i X_j are the linear, quadratic and interaction terms, respectively. The second order quadratic model used in process optimization allows the estimation of a full quadratic model for the system response [10]. However, the second order quadratic model, describing the mathematical relationship between the response (%CO degradation) and the independent variables as displayed by MINITAB 17.0 is presented in Eq. (3):

$$\%\text{ CO degradation} = 26.64 + 0.711A + 2.262B + 13.881C - 0.09427A^2 - 0.02886B^2 - 0.002922C^2 + 0.0188AB - 0.00289BC - 0.02735AC \quad (3)$$

According to Eq. (3), A, B, and, C are the coded values of the independent variables of pH, Temperature (°C) and CO concentration (g/L), respectively. The quadratic model of Eq. (3) could be used to predict the system response (%CO degradation) within the limits of the studied experimental independent variables.

Table 2. Experimental Design matrix

Run Order	Blocks	pH (A)	Temp (B)	CO Conc.(C)	% CO degradation		
					Exp.	First order	Second order
1	1	2 (1)	50 (-1)	50 (-1)	60.32	51.33	44.11
2	1	2 (1)	50 (-1)	130 (1)	53.87	49.19	42.96
3	1	10 (-1)	10 (1)	130 (1)	40.31	40.01	56.18
4	1	10 (-1)	10 (1)	50 (-1)	54.77	58.72	45.67
5	1	10 (1)	50 (1)	130 (1)	55.83	50.55	49.36
6	1	6 (0)	30 (0)	90 (0)	85.85	70.15	72.15
7	1	6 (0)	30 (0)	90 (0)	85.01	65.44	69.34
8	1	2 (-1)	10 (-1)	50 (-1)	41.81	45.06	55.43
9	1	10 (1)	50 (1)	50 (-1)	72.29	66.41	70.94
10	1	2 (-1)	10 (-1)	130 (1)	51.36	48.13	55.43
11	1	6 (0)	30 (0)	90 (0)	85.49	79.42	80.38
12	1	6 (0)	30 (0)	90 (0)	85.33	77.11	70.35
13	2	6 (-α)	60 (0)	90 (0)	70.08	65.13	75.59
14	2	6 (0)	30 (0)	90 (0)	85.63	70.66	65.37
15	2	6 (0)	7 (0)	90 (0)	41.33	36.64	49.37
16	2	6 (0)	30 (0)	24 (-α)	77.78	70.95	66.47
17	2	6 (0)	30 (0)	150 (α)	71.66	64.33	66.27
18	2	12 (0)	30 (α)	90 (0)	51.81	44.12	59.34
19	2	1.5 (0)	30 (-α)	90 (0)	40.72	47.83	56.83
20	2	6 (0)	30 (0)	90 (0)	85.11	75.44	70.16

Analytical procedure for physiochemical characterizations

The analytical methods presented in this section were used to characterize the POME, UCS, and COCS. Moisture and organic matter contents were determined using [11] and [12], respectively. The Total nitrogen was determined using the Kjeldahl method as described by [13]. The pH was determined following the method outlined by [14]. Total organic carbon (TOC) was estimated as detailed by American Public Health Association standard method [15]. Available nutrients such as calcium, sodium, magnesium potassium and phosphorous were determined according to [16]. The physiochemical characteristics of POME, UCS, and COCS are presented in Table 3.

Error analysis of the kinetic models

The accuracy of both first and second order kinetic models in explaining CO degradation process was estimated by analysing the error deviation between the experimental and model predicted values on CO degradation. The error functions from Eqs. (4) to (7) were used to estimate the errors deviations at different initial CO concentration [17]. According to Eqs (4) to (7), $Exp._i$ is the experimental value of the ith experiment; $Pred._i$ is the predicted value of the ith experiment by the model and n is the number of experiments.

$$\text{ARED} = \frac{1}{n}\sum_{i=1}^{n}\left(\frac{Exp._i - Pred._i}{Exp._i}\right) \times 100 \quad (4)$$

$$\text{RMSE} = \sqrt{\sum_{i=1}^{n}(Exp.i - Pred.i)^{2}/n} \quad (5)$$

$$\text{MAE} = \frac{i}{n}\sum_{i=1}^{n}(Exp._i - Pred._i) \quad (6)$$

$$\text{SEP} = \frac{RSME}{Exp._i} \times 100 \quad (7)$$

From Eqs (4) to (7), ARED is the Average relative error deviation, RMSE is the Root mean square error, MAE is the Mean absolute error and SEP is the Standard error of prediction.

RESULTS AND DISCUSSIONS

Physiochemical Characterization

The physiochemical properties of the UCS, COCS, and POME are summarized in Table 3. It was observed in Table 3 that POME (95.68%) contained high organic matter (OM) followed by the UCS (48.52%) and lastly the COCS (26.62%). The high OM of POME could be a source of soil nutrient and also enhance the growth of soil microbial population [18]. However, POME could also be a source of microbial biomass carbon as it contained a high level of OM [18].

The macro and micro soil nutrient compositions present in Table 3 indicated that the UCS and POME contained higher levels of calcium, potassium, and magnesium, total nitrogen, and sodium in comparison with the COCS. In terms of the organic carbon, the COCS (67.04%) showed higher level of organic carbon in comparison with the UCS (21.46%) and POME (55.5%) indicating that CO might be contributing significantly to soil organic carbon, which was needed for microbial growth [19, 20].

Furthermore, the pH values of COCS, UCS, and POME were observed to vary as the pH values for POME (5.3) and COCS (5.9) were moderately acidic. The acidic pH of POME was attributed to the organic acid produced during the fermentation process [21, 22] whereas that of COCS was due to the leaching of fundamental salt, which affects the soil pH [23]. The moderate acidic pH of COCS could be responsible for the deficiencies observed in the macro and micronutrients of the soil [24] (Table 3). The dried samples used during the physiochemical characterization test resulted in low levels of moisture content, which was observed in COCS, UCS, and POME (Table 3).

Table 3. Physiochemical properties of UCS, COCS, and POME

Parameters	Unit	UCS	COCS	POME
pH value		7.7	5.9	5.3
Organic matter	%	48.52	26.62	95.68
Total organic carbon	%	21.46	56.04	55.5
Nitrogen	%	6.09	0.82	5.7
sodium	ppm	1.13	0.24	4.66
potassium	ppm	3.16	0.37	12.4
calcium	mg/L	20.2	0.48	7.44
magnesium	mg/L	2.00	1.44	2.24
moisture content	%	11.23	6.24	12.32

Effect of POME on COCS physiochemical properties

Post characterization of the crude oil contaminated soil treated with (COCS-POME) was carried out using the standard methods in section 2.5. This was in order to investigate the effects of POME on the COCS properties after 56 days. Significant effect of POME was observed on the COCS properties except for the pH (5.9), which remained relatively within the acidic range. This might be attributed to the acidic pH (5.3) of POME prior to its addition in the COCS. Also, an increase was observed in the nitrogen level, which in turn could activate the microbial activity and increase CO degradation rate [25].

It was observed that the OM of the COCS increased after 56 days of treatment with POME. This observation indicated that the addition of POME to COCS could supply additional nutrients and also enhance microbial growth and activity [26]. Improvements were also observed in the calcium, potassium, magnesium, and sodium suggesting that POME had a stimulating effect on soil nutrients (Table 4). The diverse microbial

population in the OM rich POME could be responsible for breaking down the CO concentration.

The results obtained from the organic carbon test as presented in Table 4, showed that POME contributed to the increase in organic carbon. Accordingly, organic carbon of the COCS-POME increased by 5% compared with the organic carbon of the COCS shown in Table 3. Normally, low concentrations of raw crude oil is less volatile to atmospheric loss and could be regarded as a source of soil organic carbon for microbial growth [27, 20].

Table 4. Physiochemical Characterization of COCS-POME

Parameters	Unit	[a] COCS-POME
pH value		5.9
Organic matter	%	45.34
Total organic carbon	%	61.02
Nitrogen	%	3.92
Moisture content	%	11.09
Sodium	ppm	2.99
Potassium	ppm	1.02
Calcium	mg/L	6.14
Magnesium	mg/L	1.05

[a] COCS-POME crude oil contaminated soil treated with POME

Scanning Electron microscope (SEM)

The morphological examination of the dried POME sample was carried out using a VEGA 3 SEM. The SEM result for POME shows that the surface morphology appears to be smooth (Figure 1). This may be attributed to the presence of smooth surface particles of the POME as it was sieved after drying prior to SEM examination. The smooth surface of POME could also be attributed to the compaction and adhesion of the oil to the POME sample [28]. Also, the morphological view of POME produced by SEM showed that the porous nature of POME appears to be obvious at a magnification of 3000x and 20 µm. Furthermore, the porous nature of POME contributed significantly to the reduction in weight of the dried POME sample (Figure 1.)

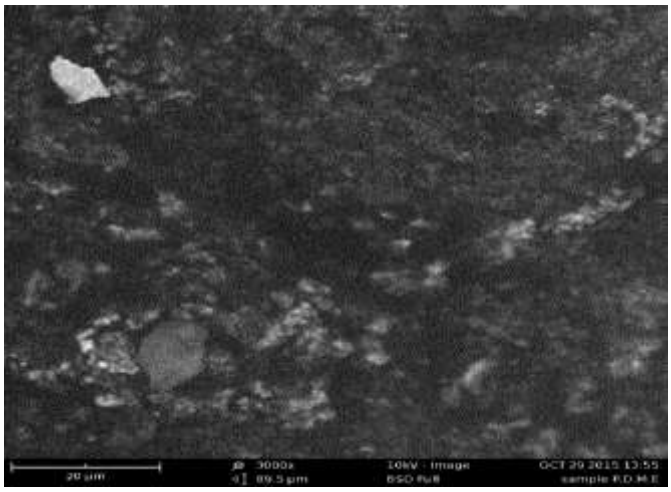

Figure 1. SEM Image of POME

FT-IR analysis of POME

The prevalent functional groups in the POME sample were identified using FT-IR (SHIMADZU, 8400S) (Figure 2). The FT-IR scan for POME sample in transmission (%) mode was in the range of 4339.02 to 396.31 cm^{-1}. The peak located at 4339.02 cm^{-1} with a transmittance of 59% was assigned to O–H stretching of oxygen. The peaks at 3827.87 to 3420.87 cm^{-1} with a transmittance of 57% and 55%, respectively are characteristics of primary amide NH_2 and phenol O-H stretching of oxygen compound. [29] reported that fat and lipids were located at 2925.15 and 2860.35 cm^{-1} with 51% transmittance (Figure 2). The peak range found at 1729.2 cm^{-1} with 55% transmittance is a characteristic of an aliphatic ketone of C=O stretching. The peaks at 1644.37 and 1534.42 cm^{-1} with 57% transmittance were nitrogen in origin (amine I and II correspondingly). [8] suggested that the IR spectrum of nitrogen band was mostly present in the form of amine. Methyl asymmetric C-H bending was observed at 1449.4cm^{-1}, with 56% transmittance [30]. The peak at 1166.97cm^{-1} with a transmittance of 56% in POME sample was assigned to lignin [31, 8]. The peaks at 440.75 and 396.31 cm^{-1} with 39% transmittance are a characteristic of P-S stretching of phosphorous compound [32]. Finally, it was obvious, that the FT-IR of POME indicated the presence of nitrogen and phosphorous compounds.

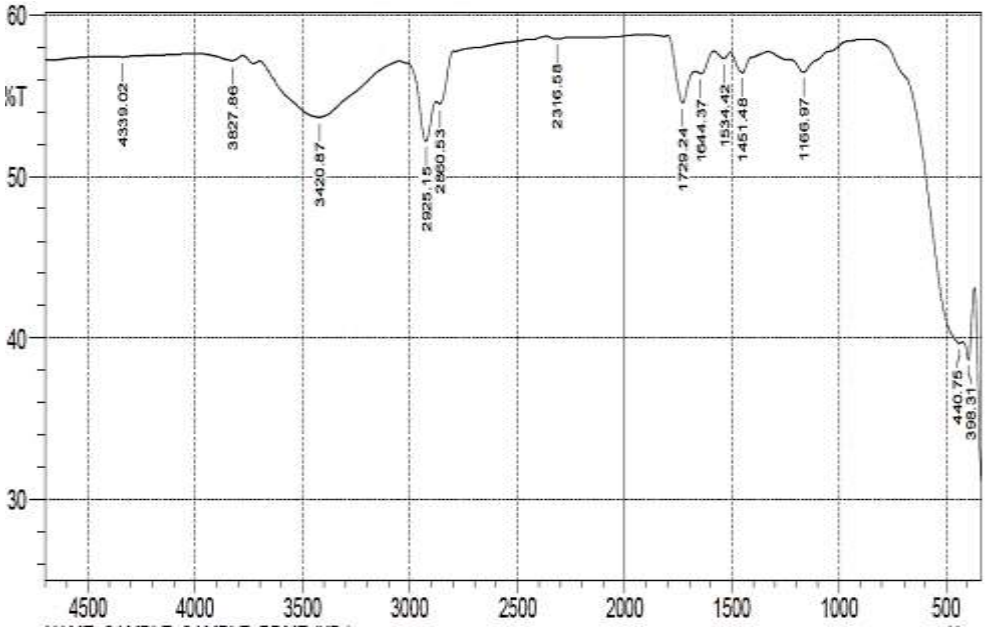

Figure 2. FT-IR spectrum for POME

Effects of initial CO concentration

Figure 3 presents the variation in results obtained for CO degradation at different initial CO concentration. It was obvious that some fractions of the CO degraded in the presence of POME as organic nutrient. However, varying rates were obtained for CO degradation at different CO concentrations (Figure 3). When comparing the CO degradation rates obtained at different CO concentrations, it was observed that 51.3% was obtained, at 130 g/L initial CO concentration (Figure 3). The CO concentration (130 g/L) could be providing enough carbon to satisfy microbial energy needs and maintenance [33]. Similarly, during the composting biodegradation of pyrene, [10] reported that a high degradation rate was achieved when high pollutant concentration is available while low concentration might not be sufficient for microbial activity [10]. Also, during the biodegradation of poly aromatic hydrocarbon (PAH), [34] reported that low PAH did not degrade in the

system even when it was supplemented with additional carbon source.

On the other hand, CO degradation rates of 35%, 29%, 22%, and 21% were obtained at 110, 90, 70, and 50 g/L, respectively (Figure 3). The CO degradation potentials of POME could be related to the high level of organic matter, which could be supplying diverse microbial population capable of degrading the CO. However, previous studies showed that microbial community was always preferable and can degrade a wide range of hydrocarbon contaminants compared with single species of microbe [35, 36]. The CO degradation might also be due to the decomposition of the biodegradable organic materials in POME with some CO fractions. However, the effect of POME on soil microbial population was not estimated, as this study focuses on the effect of POME on CO concentrations.

The CO degradation rate of 51% was considered not satisfactory, due to the fact that the utilization of POME as organic nutrient might be causing the release of toxic calcium and magnesium, which are known to harm soil microorganisms and plant (Figure 3). Another reason could be attributed to the fact that the acidic pH (5.3) of POME might not be favourable for the proliferation of soil acinetobacter, as these organisms have been identified as hydrocarbon degraders [37]. In order to counter this effect, estimates of the appropriate amount of lime required to neutralize the moderate acidic pH of POME is strongly encouraged.

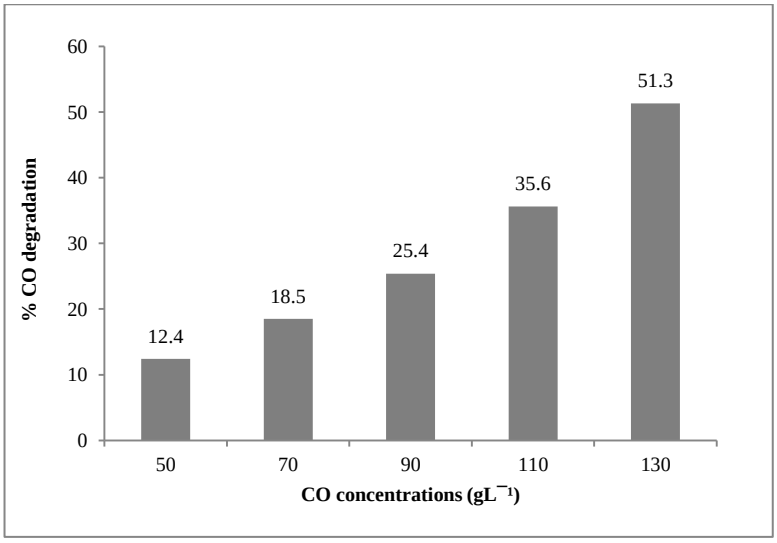

Figure 3. Effect of CO initial concentrations on CO degradation

Kinetics of CO degradation

The integrated forms of the nonlinear first and second order kinetic models in Table 5 were used to estimate the rate constants (K) at different initial CO concentrations. Where [Co] and [Ct] are the initial and final CO concentrations in the soil at time t = 0 and t = t, respectively, and t is the time in days. The kinetic parameters in Table 6 were estimated from the nonlinear first and second order kinetic using the Microsoft excel solver function according to [38].

Table 5. CO degradation kinetic models

Models	Equations	Plots
First order	$[Ct] = [Co]e^{-K_1 t}$	[Ct] vs t
Second order	$[Ct] = \frac{1}{K_2.t + \frac{1}{[Co]}}$	[Ct] vs t

The variations in the degradation of CO concentrations for first and second order are shown in Figure 4 (a to e). It was evident from the plots in Figures 4(a to e) that the CO concentrations approaches zero more slowly in the second-order, in comparison with the first order. These observations indicated that the first order CO

degradation kinetic model results in a nearly complete degradation of the CO contaminant.

After 56 days, the first order CO degradation rates constants of 0.0119, 0.0117, 0.0141, 0.0159, and 0.0165 day^{-1} were obtained (Table 6). These values correspond to the initial CO concentrations of 50, 70, 90, 110, and 130 g/L, respectively. The second order CO degradation rate constants at the same initial CO concentrations were 0.00025, 0.00020, 0.00016, 0.00015 and 0.0117 day^{-1}. Despite the low intrinsic rate constants generally observed, the first order rate constants were higher compared with the second order. Similarly, the addition of nitrogen and phosphorous amendments in total petroleum hydrocarbon (TPH) contaminated soil, resulted in TPH biodegradation rate constants of 0.011 to 0.018 day^{-1} [39].

The biological half-lives for CO degradation at different initial CO concentrations were calculated for first and second order kinetic models using Eqs. (8) and (9), respectively. For a first order kinetic model, the half-life is inversely related to the first order rate constant (k_1) as expressed in Eq. (8). While for a second-order kinetic model, the half-life is inversely related to the initial CO concentration and the second order rate constant (k_2) as expressed in Eq. (9):

$$T_1^{1/2} = \frac{\ln 2}{k_1} \quad (8)$$

$$T_2^{1/2} = \frac{1}{k_2[Co]} \quad (9)$$

The first order biological half-lives corresponding to the initial CO concentrations of 50, 70, 90, 110 and 130 g/L were 56, 54, 49, 43, and 42 days, respectively (Table 6). However, the second order biological half-lives at the same initial CO concentrations were 80, 71, 69, 60, and 45 $g/L.day^{-1}$. These observations indicated that the biological half-lives were longer at low CO concentrations. However, the second order half-lives were higher than the first order at all initial CO concentrations indicating that the CO degradation in the COCS according to second-order kinetics might be very slow.

Table 6. Kinetic parameters for CO degradation at different CO concentrations

Parameters	CO concentrations (gL^{-1})				
	50	**70**	**90**	**110**	**130**
First order					
K_1 (day^{-1})	0.0122	0.0127	0.0141	0.0159	0.0165
T½ (days)	56	54	49	43	42
R^2	0.966	0.992	0.971	0.962	0.987
Second order					
K_2 (day^{-1})	0.00025	0.00020	0.00016	0.00015	0.00017
T½ ($g/L.day^{-1}$)	80	71	69	60	45
R^2	0.844	0.911	0.853	0.902	0.923

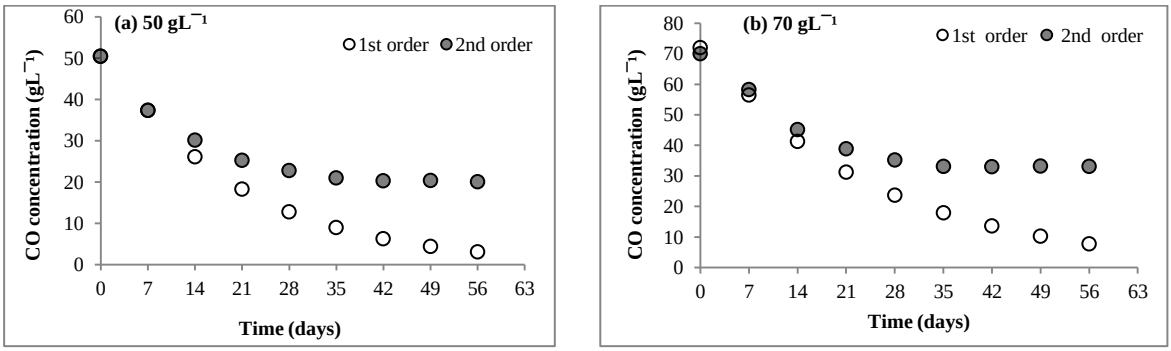

Figure 4. 4a to 4e. Non-linear first and second order plots for CO degradation.

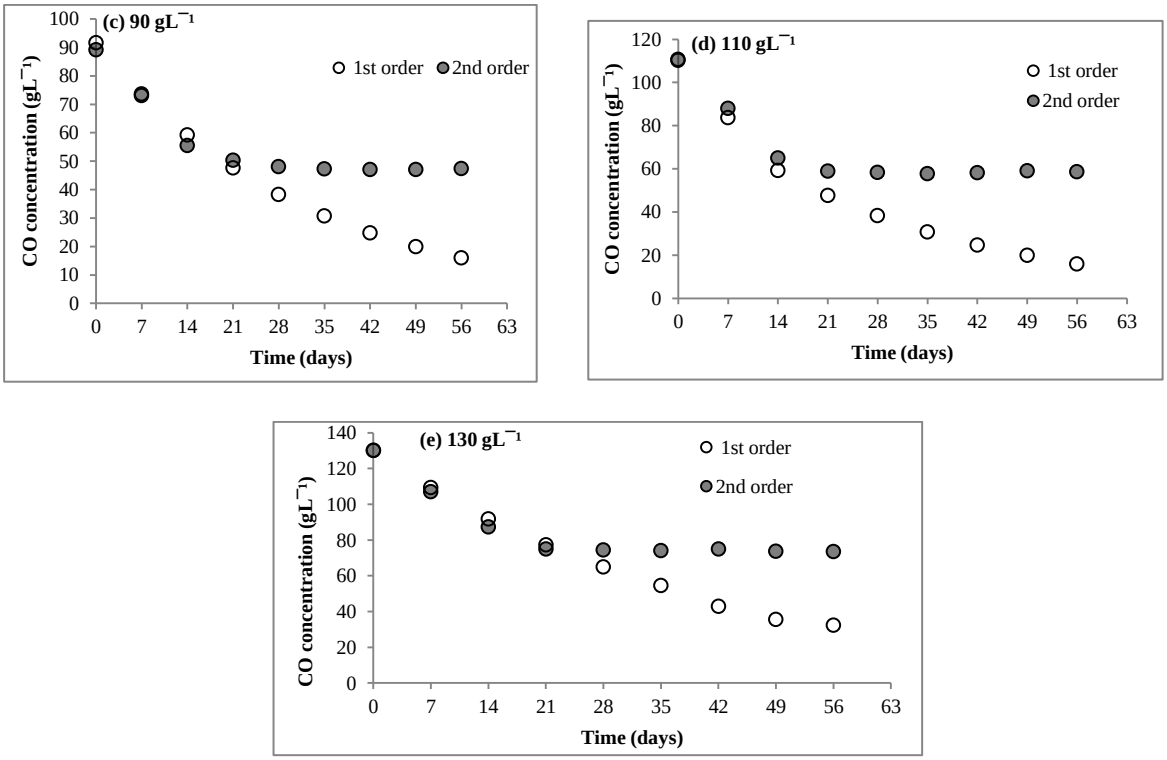

Figure 4. Continued.

Error estimations for first and second order models

Both first and second order models were compared for their predictive capability on CO degradation. The experimental values as well as the values obtained using first and second order models are presented in Table 2. However, error analysis using statistical error functions such as ARED, RMSE, MAE, and SEP as presented in Eqs. (4) to (7), were used to compare the results between the experimental and first and second order models. The results of the statistical error analysis at different initial CO concentration [17] for first and second order model are listed in Table 7.

However, lower values of the Average relative error deviation (ARED), Root mean square error (RMSE), Mean absolute error (MAE), and Standard error of prediction (SEP) were obtained for first order at all initial CO concentration indicating a higher predictive accuracy of the first order model (Table 7). [40] reported that the lower the values of error analysis the better the goodness of fit of the model. Similarly, [41] demonstrated that the lowest values of root mean square error (RMS), sum of absolute error (EABS) and average relative error (ARE) were obtained when the total petroleum hydrocarbon (TPH) was modelled using first order kinetic model. Also, previous studies reported the accuracy of TPH modelling using the first order kinetic model as the contaminant degradation was inversely proportional to its concentration [42].

Table 7. Kinetic error deviation data at different initial CO concentration

Kinetic models	RMSE	ARED	MAE	SEP
		50g/L		
First order	0.057731	0.02788	2.82945	1.719186
Second order	0.874881	2.02176	7.535176	4.96045
		70g/L		
First order	0.118588	0.997014	2.101729	4.291186
Second order	0.694602	4.78976	3.965301	14.09257

Table 7. Continued

			90g/L		
First order	0.587441	1.683001		1.775002	2.87586
Second order	1.881634	2.94057		5.764321	6.778613
			110g/L		
First order	0.41381	5.96426		2.85919	5.03452
Second order	0.570069	8.79331		7.636318	10.60316
			130g/L		
First order	0.643771	5.163387		2.077854	2.224611
Second order	0.993276	8.593211		9.226021	12.11765

ANOVA for the quadratic model

The lack of fit test, *P*-value, and R^2 in the ANOVA Table 8 were used to check the significance of the quadratic model. The diagnostic test of the lack of fit compares both the residual and pure errors from a replicated experimental design point [43]. The R^2 measures the degree of total variability explained by the quadratic model. However, *P*-value of lack of fit if greater than 0.05 clearly showed the non-significant lack of fit [43]. A non-significance lack of fit suggests the suitability of the model and the significant effect of the independent variables on the response [44].

From the ANOVA Table 8, the *P*-value and *F*-value for the lack of fit were 0.260 and 8.17, respectively. These values indicated that the model lack of fit was non-significant, which confirmed the adequacy of the quadratic model in explaining the effects of the independent variables on the response. From the *P*-values in the ANOVA Table 8, it was found that the independent variables of A, B, C, A^2, B^2, C^2, BC, and AC were significant model terms ($P < 0.05$). Hence, eliminating the non-significant variable (AB), from Eq. (3), the final significant quadratic model of Eq. (10) was obtained.

$$\% \text{ CO degradation} = 26.64 + 0.711A + 2.262B + 13.881C - 0.09427A^2 - 0.02886B^2 - 0.002922C^2 - 0.00289BC - 0.02735AC \quad (10)$$

Eq. (10) was used to study the interactions between the independent variables and the response. The contributions of the independent variables of the quadratic model were important in order to understand the influence of each of them during the CO degradation process. Therefore, ANOVA of MINITAB 17.0 was used to calculate the percentage contributions of the independent variables presented in Table 8.

Accordingly, the independent variables of A^2 and B^2 in the quadratic term of the model were more influential. These independent variables contributed 50.13% and 24.22%, respectively. The independent variables of A and B in the linear term contributed 13.25% and 1.86% respectively. The two-way interactions between the independent variables of AB and BC contributed 1.50% and 0.70%, respectively.

[45] noted that by studying the main effects and contributions of each variable, the studied process could be characterized and predicted. Consequently, the quadratic model in the ANOVA Table 9 was the primary determining factor for the CO degradation with 78.8%. The linear and two-way interactions had the least contributions, accounting for 16.6% and 3.52%, respectively (Table 8).

The values of the adjusted coefficient of determination (R^2 Adj) and the predicted coefficient of determination (R^2 Pred) were 97.96% and 89.64%, respectively, indicating a high correlation between the observed and predicted values of the quadratic model. From Table 9, the optimize results obtained were in good agreement with the model actual solution, which confirmed the validity of the quadratic model.

Table 8. ANOVA for the response surface quadratic model

Source	DF	Seq SS	Contribution%	Adj SS	Adj MS	F-value	P-value
Model	10	5720.22	99.03	5720.22	572.02	92.36	0.000
Blocks	1	6.48	0.11	6.48	6.48	1.05	0.333
Linear	3	958.89	16.6	958.89	319.63	52.61	0.000
A- pH	1	86.44	13.25	765.21	765.21	123.55	0.000
B-Temp	1	765.21	1.86	86.44	86.44	13.96	0.005
C-CO conc.	1	107.24	1.5	107.24	107.24	17.32	0.002
Quadratic	3	4551.62	78.8	4551.62	1517.21	244.97	0.000
A^2	1	1399.18	50.13	1759.88	1759.88	284.15	0.000
B^2	1	2895.22	24.22	3004.73	3004.73	485.15	0.000
C^2	1	257.21	4.52	257.21	257.21	41.53	0.000
2-way interaction	3	203.23	3.52	203.23	67.74	10.94	0.002
AB	1	18.06	1.50	18.06	18.06	2.92	0.122
BC	1	40.50	0.70	40.50	40.5	6.54	0.031
AC	1	144.67	0.13	144.67	144.67	23.36	0.001
Error	9	55.74	0.97	55.74	6.19		
Lack-of-fit	5	55.24	0.96	55.24	11.05	8.17	0.260
Pure Error	4	0.50	0.01	0.50	0.13		
Total	19	5775.96	100				
	R^2	R^2 (Adj)	PRESS	R^2 (Pred)			
Model Summary	99.03%	97.96%	58.404	89.64%			

Table 9. Response Optimization

Variables	Starting values	Optimized solution	Response prediction (Optimized values)
Temp (°C)	7.11	35.58	30.5
CO Conc. (g/L)	24.75	71.35	75
pH	1.571	6.12	6
%CO degradation		78.036	78.4

Response surface plots

The graphical representation of the quadratic model was in form of the 3D response surface. These plots showed the interactions of the independent variables at different levels for the studied CO degradation using POME. It was observed from the 3D surface plots in Figures. 5, 6 and 7, that a temperature and pH of 30°C and 7, respectively with CO concentration of 75 g/L increased CO degradation. Similarly, [46] observed an increase in atrazine degradation from a temperature of 20 °C to 29.3°C and pH 6.7 using microbial mixed culture. However, they noted that with further increase in temperature and pH, atrazine degradation decreased and was attributed to the loss of the viable microbial cell.

Furthermore, experimental validation of the model prediction in Table 9 was carried out using the optimized conditions of pH (6); temperature (30.5^{o}C) and CO concentration (75 g/L). A maximum CO degradation of 71.3% ± 0.043 was achieved. The satisfactory agreement between the predicted (78.4%) and the experimental result (71.3%) on CO degradation validated the optimal values. These results further showed that the quadratic model correctly explains the influence of the chosen independent variables on CO degradation using POME.

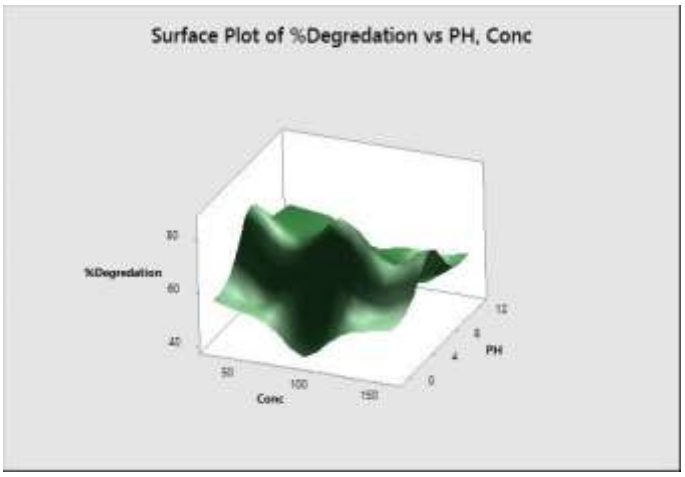

Figure 5. 3D surface plot of pH and Concentration

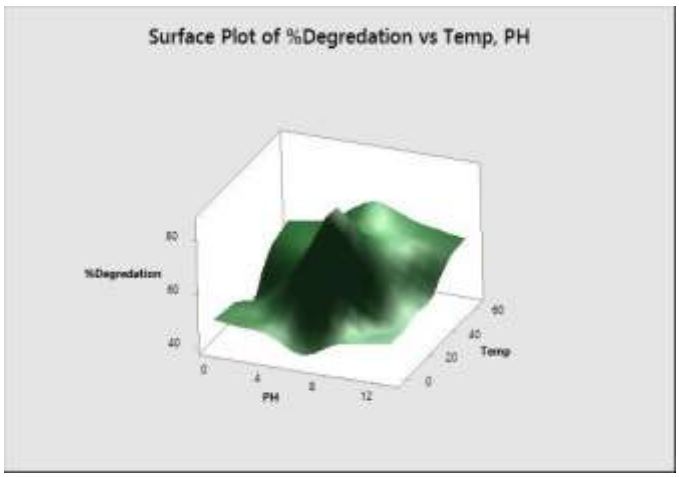

Figure 6. 3D surface plot of Temperature and pH

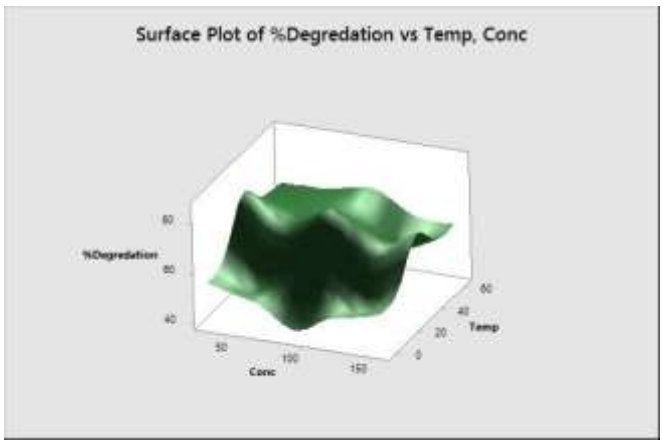

Figure 7. 3D surface plot of Temperature and Concentration

CONCLUSIONS

In this study, the effects of process parameters on crude oil biodegradation of POME using response surface optimization were investigated. From the effects of POME on initial CO concentrations, it was observed that higher CO degradation rates were obtained at 130 g/L initial CO concentration. Furthermore, this study also revealed the potentials of POME as organic manure. This was due to the fact that some of the scarce nutrients in the COCS were restored after 56 days of treatment with POME. The first order kinetic model proved a better model with higher degradation rate constants and lower biological half-lives. The RSM optimization process showed that the optimum condition for CO degradation using POME was CO concentration (75 g/L), temperature (30.5°C) and pH (6) with CO degradation efficiency of 78.04%. From the ANOVA results, the quadratic model significantly contributed to the CO degradation process with 78.8%. The results obtained from this study suggest that POME can be used as organic manure in COCS.

ACKNOWLEDGEMENTS

The authors would like to thank the authorities of Nnamdi Azikiwe University Awka, Anambra State Nigeria and University of Nigeria Nsukka Enugu State for providing the necessary facilities for this research work.

Conflict of Interest

Authors declare that no conflict of interest exists.

REFERENCES

1. Rupani P. F., Singh R. P., Ibrahim H., Eas N., 2010. Review of current palm oil mill effluent treatment methods. J World Appl Sci. 11, 70 – 81

2. Madaki S.Y., Seng L., 2013. Palm oil mill effluent (POME) from Malaysia palm oil mill; waste or resource, Inter J Environ Technol. 2, 1138 - 1155

3. Bhatia S., Othman Z., Ahmad A. L., 2007. Coagulation-flocculation process for POME treatment using Moringa oleifera seeds extract: Optimization studies. Chem Eng J. 133, 205 – 212

4. Wu T.Y., Mohammad A.W., Jahim J.M., Anuar N., 2007. Palm oil mill effluent (POME) treatment and bio resources recovery using ultrafiltration membrane: effect of pressure on membrane fouling. Biochem Eng J. 35, 309 – 317

5. Khalid A.R., Mustafa W.A.W., 1992. External benefits of environmental regulation: Resource recovery and the utilization of effluents. The Environmentalist, 12, 277 – 285. doi.org/10.1007/BF01267698.

6. Oviasogie P.O., Aghimien A.E., 2003. Micronutrient status and speciation of copper, iron, zinc and zinc in soil containing palm oil mill effluent. Global J Pure and Appl Sci. 9, 71 – 80

7. Wu T.Y., Mohammad A.W., Jahim J.M., Anuar N., 2009. A holistic approach to managing palm oil mill effluent (POME): Biotechnological advances in the sustainable reuse of POME, Biotechnol Adv. 27, 40 – 52. doi: 10.1016/j.biotechadv.2008.08.005

8. Baharuddin A. S., Wakisaka M., Shirai Y., Abd Aziz S., Abdul Rahman N. A., Hassan M. A., 2009. Co-Composting of empty fruit bunches and partially treated palm oil mill effluent in a pilot scale. Inter J Agric Resource. 4, 69 -78

9. Peressutti S.R., Alvaerz H.M., Pucci O.H., 2003. Dynamics of hydrocarbon degrading bacteriocenosi of experimental oil pollution in Patagonian soil, Inter J Bio-deterior Biodegra. 52, 21 – 30.

10. Sayara T., Sarra M., Sanchez A., 2010. Optimization and enhancement of soil Bioremediation by composting using experimental design technique. Biodegrad. 21, 345 – 356

11. American society for testing and materials (ASTM) D4643- 2013. Determination of soil moisture content, US Department of Agriculture.

12. American society for testing and materials (ASTM) D2974- 2014. Determination of soil organic matter contents of soil by Microwave oven heating, US Department of Agriculture.

13. Rutherford P. M., McGill W.B., Arocena J.M., Figueiredo C.T., 2008. Total Nitrogen Soil Sampling and Methods of Analysis, Canadian Society of Soil Science, 3rd Edition, Taylor & Francis Group for CRC Press.

14. American society for testing and materials (ASTM) D4972- 2013. Standard Test Method for pH of Soils, ASTM International, West Conshohocken, www.astm.org doi: 10.1520/D4972.2013

15. American Public Health Association APHA, 2005. Standard method for the determination of water and wastewater, 21st Edition, Total organic carbon (TOC): high temperature combustion method (5319A and 5310B).

16. US Department of Agriculture and the US composting council 2001. Test methods for the determination of available nutrients in compost, Edaphos, International Houston.

17. Riahi K., Safa C., Bechir B.T., 2013. AKinetic modelling study of phosphate adsorptiononto phoenix dactylifera L date palm fibre inbatch mode. J Saudi Chem Soci. In Press.

18. Sayara T., Sarra M., Sanchez A., 2009.Preliminary screening of co substrate for bioremediation of pyrene contaminated soil through composting. J Hazard Mater. 172, 1695-1698

19. Bundy J.G., Paton G.I., Campbell C.D., 2002. Microbial communities in different soiltypes do not converge after diesel contamination. J Appl Microbiol. 92, 276 – 288

20. Alrumman A., Standing D.B., Paton I., 2014. Effect of hydrocarbon contamination on soil microbial community and enzyme activity. J King Saudi Uni. 27, 31- 41

21. Habib M.A.B., Yusoff S.M., Phang K.J., Mohamed S., 1997. Nutritional value ofchironomid larvae grown in palm oil mill effluent and algal culture. Aquaculture. 158, 95-105

22. Muhrizal S.J., Shamshuddin I., Fauziah M.A., Husni H., 2006. Changes in iron ore pooracid sulphate soil upon submergence Geothermal. 131, 110-122.

23. United State department of Agriculture, Natural Resource Conservation Service (USDA, NRCS) Soil quality kit-guide for educators 2001.

24. Cheraghi M., Sobhanardakani S., Lorstani B., Merrikhpour H., Mosaid H. P., 2015. Biochemical and physical characterization of petroleum hydrocarbon contaminated soil in Tehran. J Chem Health Risks. 5, 199-208

25. Margesin R., Schinner F., 2000. Bioremediation (Natural Attenuation and bio Stimulation) of diesel oil contaminated soil in Apline Glacier skiing area. Appl Environ Microbiol. 67, 3127 - 3133

26. Xu R., Obbard J.P., 2003. Effect of nutrient amendment on indigenous hydrocarbon biodegradation in crude oil contaminated beach sediments. J Environ Quality. 32, 1234 - 1243.

27. Marinescu M., Toti M., Tanase V., Plopeanu G., 2011. Effect of crude oil pollution on physical and chemical characteristics of soil. Res J Agric. 43, 125 – 129

28 Alrawi R.A., Ab Rahman N.N.N., Ahmad A., Ismail N., Mohd Omar A. K., Characterization of oily and Non-Oily Natural Sediments in palm oil mill effluent. doi.org/10.1155/2013/298958.

29. Grube M., Lin J.G., Lee P.H., Kokorevicha S., 2006. Evaluation of sewage sludge based compost by FT-IR spectroscopy. African J Geo-Chem. 130, 324 - 333

30. Giovanela M., Parlanti E., Sierra S.J., Soldi M.S., Sierra M.D., 2004. Elemental composition FT-IR spectra and thermal behaviour of sedimentary fulvic and humic acid from aquatic and terrestrial environment. J Geo Chem. 38, 255-264

31. Matias M.C., Orden M.U., Sanchez C.G., Urreaga J.M., 2000. Comparative spectroscopy study of modification of cellulose material with different coupling agents. J Appl Poly Sci. 75, 256 – 266

32. Stuart H.B., 2004. Infrared spectroscopy, fundamentals and applications, University of Technology Sydney Australia John Wiley & Sons Ltd.

33. Gailute I., Rackauskiene G., Grigiskis S., 2014. Changes in crude oil hydrocarbon degradation by Arthrobacter Sp. MI and Acinetobacteria Pr82 in selected optimal condition, Biologija. 60, 134 – 141

34. Zappi M.E., Rogers B.A., Teeter C.I., Gunnison D., Bajpai R., 1996. Bio-slurry treatment of soil with low concentration of total petroleum hydrocarbon. J Hazard Mater. 46, 1-12

35. Roling W.F., Milner M.G., Jones D.M., Lee K., Daniel F., Swannell R. J., Head I. M., 2002. Robust hydrocarbon degradation and dynamics of bacterial community during nutrient enhanced oil spill

bioremediation. Appl Environ Microbiol. 68, 5537 – 5548

36. Yong-Chao G., Shu-hai G., Jia-ning W., Li D.,Wang H., De Hui-Zang., 2014. Effect of different remediation treatments on crude oil contaminated saline soil. Chemosphere. 117, 486-493

37. Tanase A.M., Csutak V.T., Pelinesu D., Robertina I., Stoica I., 2012. Phylogenetic analysis of oil polluted soil microbial strain, Romania Biotechnol Lett, 17, 7093 - 7103

38. Hossani A.M., Ngo H.H., Guo W., 2013. Introductory of Microsoft Excel SOLVER Function spread sheet method for isotherm and kinetics modelling of metals biosorption in waste water. J water Sustainability. 3, 223 – 237

39. Chang W., Dyen M., Spagnuolo L., Simon P., Whyte L., Ghoshal S., 2010. Biodegradation of semi and non- semi petroleum hydrocarbon in aged contaminated soil from Sub-Arctic ice. Chemosphere. 80, 319 – 326

40. Kitanovic H.S., Milenovic D., Veeljkovic V.B., 2008. Empirical kinetic models for the resinoid extraction from aerial parts of Saint John's Wort (*Hypericum perforatum* L.) Biochem Eng. 41, 1-11

41. Farahat L.A., El-Gendy N.S., 2007. Comparative kinetic study of different bioremediation Process for soil contaminated with petroleum hydrocarbon. J Mater Sci Res India. 4, 269-278.

42. Jorgensen K.S., Puustinen J Suortti, 2000. Bioremediation petroleum hydrocarbon contaminated soil by composting biopile. J Environ Pollut. 107, 245-254

43. Gomez F., 2014. Assessment and Optimization of Ex-Situ Bioremediation of Petroleum contaminated Soil under Cold Temperature Conditions, M.Sc. Thesis, University of Ottawa Canada.

44. Shahavi M.H., Morteza H., Mohsen J., Ghasem N., 2015. Optimization of encapsulated clove oil particle size with biodegradable shell using design expert methodology. Pakistan J Biotechnol. 12, 149 - 160

45. Myers R.H., Montgomery D.C., Anderson-Cook C.M., 2009. Response Surface Methodology: Product and Process Optimization Using Designed Experiments. 3rd Edition, John Wiley & Sons, New York.

46. Debamista N., Rajasimman M., 2013. Optimization and Kinetics study on Biodegradation of atrazine using mixed microorganisms. Alexandria Eng J. 52, 499 – 505.